Phospholipid Subclass-Specific Alterations in the Kinetics of Ion Transport across Biologic Membranes†

Xi Chen and Richard W. Gross*

Division of Bioorganic Chemistry and Molecular Pharmacology, Departments of Medicine, Chemistry and Molecular Biology & Pharmacology, Washington University School of Medicine, St. Louis, Missouri 63110

Received April 25, 1994; Revised Manuscript Received July 18, 1994®

ABSTRACT: Although the predominance of plasmalogens in electrically-active membranes (e.g., sarcolemma) is well-known, identification of the molecular mechanisms through which the vinyl ether linkage facilitates electrophysiologic function has remained elusive. Herein we demonstrate that the kinetics of both carrier-mediated (i.e., valinomycin) and passive ion transport are substantially different in membranes comprised of plasmalogen molecular species in comparison to their diacyl and alkyl ether choline glycerophospholipid subclass counterparts. The rank order of valinomycin-mediated K^+/Na^+ exchange in membranes comprised of each choline glycerophospholipid subclass was plasmenylcholine ($\kappa = (6.1 \pm 0.7) \times 10^{-2}$ s^{-1}) > plasmanylcholine ($\kappa = (1.9 \pm 0.2) \times 10^{-2}$ s^{-1}) ≅ phosphatidylcholine ($\kappa = (2.3 \pm 0.5) \times 10^{-2}$ s^{-1}). A similar hierarchy of rate constants for valinomycin-facilitated Na^+ transport in each subclass was manifest. In contrast, the phospholipid subclass rank order for passive Cl^- flux was phosphatidylcholine ($\kappa = (2.6 \pm 0.4) \times 10^{-4}$ s^{-1}) > plasmanylcholine ($\kappa = (0.8 \pm 0.1) \times 10^{-4}$ s^{-1}) ≅ plasmenylcholine ($\kappa = (0.6 \pm 0.2) \times 10^{-4}$ s^{-1}). Based upon known diferences in the conformation, dynamics, membrane dipole potential, and electron-donating properties of these choline glycerophospholipid subclasses, a model is presented which explains the subclass-induced differences in carrier-mediated and passive ion transport providing a rationale for the predominance of plasmalogens in electrically-active membranes.

Biologic membranes are comprised of distinct phospholipid subclasses (Figure 1) whose relative composition, subcellular compartmentation, and complement of individual molecular species are strictly maintained through highly-conserved regulatory processes (e.g., Ramesha & Pickett, 1987; MacDonald & Sprecher, 1989; Tshinaga et al., 1991; Johnston & Goldfine, 1992; Bayon et al., 1993). Despite the presence of substantial amounts of cellular enzymic machinery dedicated to the maintenance of a precisely−tailored phospholipid subclass composition in each individual subcellular membrane compartment in mammalian cells, the reasons underlying the heterogeneity of phospholipid subclasses in mammalian membranes have remained enigmatic (Karnovsky et al., 1982; Shaikh, 1990; Takamura et al., 1990; Masuda et al., 1991; Gross, 1992).

Recently, we demonstrated that plasmalogens are the predominant phospholipid constituents in the electrically-active membrane of cardiac myocytes (i.e., sarcolemma) and that the molecular dynamics and conformation of plasmenylcholine are distinct from their diacyl phospholipid counterparts (Gross, 1984, 1985; Pak et al., 1987; Han & Gross, 1990). On the basis of these observations, we hypothesized that one reason underlying the predominance of plasmalogens in electrically-active tissues was their ability to differentially modulate the kinetics of ion transport by virtue of their substantially different molecular geometry, dipole potential, and intrinsically disparate electron-donating properties at the hydrophobic−hydrophilic interface in comparison to diacyl phospholipids. We now report that the covalent linkage present in the proximal portion of the *sn*-1 phospholipid constituent (i.e., the phospholipid subclass) is an important determinant of the kinetics of valinomycin-mediated ion transport as well as passive ion transport across membrane bilayers.

MATERIALS AND METHODS

Materials. 1-Hexadecanoyl-2-eicosa-5′,8′,11′,14′−tetraenoyl-*sn*-glycero-3-phosphocholine (phosphatidylcholine) and bovine heart lecithin were obtained from Avanti Polar Lipids, Inc. (Alabaster, AL). Arachidonoyl chloride was purchased from Nu Chek Prep, Inc. (Elysian, MN). Fluorescent probes 3,3′-dipropylthiadicarbocyanine iodide (diS-C_3-(5)[1]), 1,7-diaza-4,10,13-trioxacyclopentadecyl benzofuranyl isophthalate (SBFI), and 1,10-diaza-4,7,13,16-tetraoxacyclooctadecyl benzofuranyl isophthalate (PBFI) were supplied by Molecular Probes, Inc. (Eugene, OR). Valinomycin, monensin, gramidicin, and most other chemicals were obtained from Sigma Chemical Co. (St. Louis, MO).

Synthesis of Ether Phospholipids. 1-*O*-(*Z*)-hexadec-1′-enyl-*sn*-glycero-3-phosphocholine (lysoplasmenylcholine) was

† This research was supported by NIH Grant No. 34839.

* Author to whom correspondence should be addressed: Richard W. Gross, M.D., Ph.D., Division of Bioorganic Chemistry and Molecular Pharmacology, Washington University School of Medicine, 660 South Euclid, Box 8020, St. Louis, MO 63110. Telephone Number 314-362-2690. FAX Number 314-362-1402.

® Abstract published in *Advance ACS Abstracts,* October 15, 1994.

[1] Abbreviations: diS-C_3-(5), 3,3′-dipropylthiadicarbocyanine iodide; SBFI, 1,7-diaza-4,10,13-trioxacyclopentadecyl benzofuranyl isophthalate; PBFI, 1,10-diaza-4,7,13,16-tetraoxacyclooctadecyl benzofuranyl isophthalate; plasmanylcholine, 1-*O*-hexadecyl-2-eicosa-5′,8′,11′,14′-tetraenoyl-*sn*-glycero-3-phosphocholine; plasmenylcholine, 1-*O*-(*Z*)-hexadec-1′-enyl-2-eicosa-5′,8′,11′,14′-tetraenoyl-*sn*-glycero-3-phosphocholine; phosphatidylcholine, 1-hexadecanoyl-2-eicosa-5′,8′,11′,14′-tetraenoyl-*sn*-glycero-3-phosphocholine; lysoplasmenylcholine, 1-*O*-(*Z*)-hexadec-1′-enyl-*sn*-glycero-3-phosphocholine; TLC, thin layer chromatography.

0006-2960/94/0433-13769$04.50/0

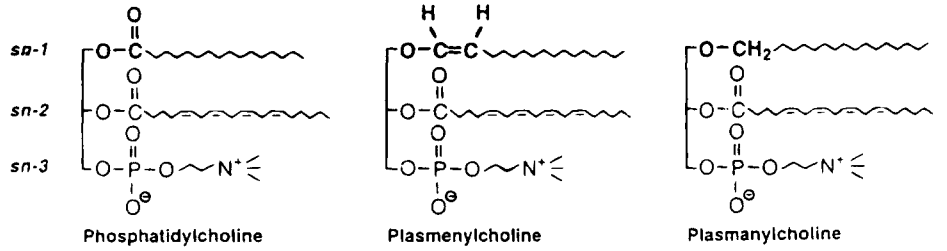

FIGURE 1: Choline glycerophospholipid subclasses containing arachidonic acid at the *sn*-2 position. Phospholipid subclasses are categorized by the nature of their covalent attachment to the *sn*-1 glycerol hydroxyl group and include ester, vinyl ether, or alkyl ether linkages which in the case of choline glycerophospholipids correspond to phosphatidylcholine, plasmenylcholine, and plasmanylcholine, respectively. Phospholipid subclasses utilized in this study contained arachidonic acid at the *sn*-2 position as indicated.

prepared by alkaline methanolysis of bovine heart choline glycerophospholipids and purified by straight- and reverse-phase HPLC as previously described (Creer & Gross, 1985; Han et al., 1992). Choline ether glycerophospholipid subclasses were synthesized using lysoplasmenylcholine or lysoplasmanylcholine as precursors by condensation with arachidonoyl chloride utilizing catalytic amounts of dimethylaminopyridine (Han et al., 1992). The resultant 1-*O*-(*Z*)-hexadec-1′-enyl-2-eicosa-5′,8′,11′,14′-tetraenoyl-*sn*-glycero-3-phosphocholine (plasmenylcholine) or 1-*O*-hexadecyl-2-eicosa-5′,8′,11′,14′-tetraenoyl-*sn*-glycero-3-phosphocholine (plasmanylcholine) was purified by straight-phase HPLC (Han et al., 1992), and its purity was substantiated by electrospray ionization−mass spectrometry (ESI−MS), which demonstrated a single intense peak for each synthetic ether glycerophospholipid.

Fluorescence Measurements of Valinomycin-Mediated Potential Dissipation. Fluorescence intensities of diS-C_3-(5) were measured utilizing an SLM spectrofluorometer 4800C (SLM Instruments, Urbana, IL) employing an excitation wavelength of 622 nm (2 nm slit width) and an emission wavelength of 670 nm (8 nm slit width). Small unilamellar vesicles (d = 30 nm) comprised of each phospholipid subclass in K^+ medium (225 mM K_2SO_4, 50 mM KH_2PO_4−K_2HPO_4, pH 6.7 at 25 °C) were prepared by high-energy sonication (Vibra Cell Model VC600 sonicator) under a N_2 atmosphere (two 3.5 min bursts at a power level of 1 employing a 30% duty cycle with cooling at 0 °C between sonication periods) (Chen et al., 1993). The resultant lipid suspension was centrifuged for 10 min at 30000g_{max} to remove undispersed residue prior to the passage of the unilamellar vesicles through a G-25 Sephadex column equilibrated with the same K^+ medium in which they were prepared. The peak fraction of the liposome eluate was diluted with Na^+ buffer (225 mM Na_2SO_4, 50 mM NaH_2PO_4−Na_2HPO_4, pH 6.7 at 25 °C) or isoosmotic Li^+ buffer (266 mM Li_2SO_4, 18 mM LiCl, pH 6.7 at 25 °C) resulting in the generation of an inward 100 mV potential after addition of valinomycin ($E = RT/F \ln([K^+]_{out}/[K^+]_{in})$. A 2-mL volume of diluted liposome solution (~50 μg/mL) was added to a cuvet and equilibrated to 25 °C. DiS-C_3-(5) from a stock ethanol solution (final dye concentration 1.0×10^{-6} M) was added directly to the stirred suspension while emission intensity was recorded as a function of time. Three minutes after the addition of the dye, the fluorescence intensity reached a plateau, which was assigned a relative value of 1.0. At this time, valinomycin in ethanol (final concentration 1.0×10^{-6} M) was added to hyperpolarize the vesicles, and the fluorescence intensity was further recorded for ≈ 7 min. The ethanol concentration in the vesicle suspension never exceeded 0.7%. Initial rate constants (κ) of K^+ efflux were calculated from the slope of initial potential dissipation assuming that the membrane potential was controlled by both K^+ and Na^+ gradients across the membrane in the presence of valinomycin and that the dye fluorescence change was proportional to the membrane potential change during the initial time period (Corda et al., 1982). By differentiation of the Goldman−Hodgkin−Katz equation, we obtain

$$k_{slope} = \frac{dE}{dt} \approx -\frac{RT}{F}\frac{d \ln[k_1 - k_2 (C_0 - C)]}{dt}$$

where k_{slope} is the slope of initial potential dissipation, E is the membrane potential, k_1, k_2 are constants, and C_0, C are the potassium ion concentration at time 0 and t, respectively, in the intravesicular space. The above equation can be further integrated using the initial conditions of potential dissipation as

$$C_0 - C = \frac{k_1}{k_2}(1 - e^{-[k_{slope}/(RT/F)]t})$$

where $C_0 - C$ represents the initial concentration change in the intravesicular space due to K^+ efflux in exchange for Na^+ and $k_{slope}/(RT/F)$ is the apparent K^+/Na^+ exchange rate constant (κ) which is rate-limited by Na^+ influx. No detectable degradation of phospholipids during the time course of the experiment was found as ascertained by TLC using a mobile phase of $CHCl_3$/MeOH/NH_4OH (65/25/5, v/v/v) and subsequent intense iodine staining.

Valinomycin-Mediated Na^+ or Cl^- Flux. Dried phospholipid films were hydrated in buffer (300 mM $(CH_3)_4NCl$, 10 mM MOPS, 5 mM Tris·Cl, 0.01 mM EDTA, pH 7.0 at 25 °C) containing either 300 μM SBFI (Na^+ mobility measurement) or PBFI (Cl^- permeability measurement) prior to vortex mixing. Large unilamellar vesicles (d = 100 nm) were subsequently obtained by lipid extrusion through polycarbonate membranes by repetitive extrusion of liposomes as previously described (Hope et al., 1985). Nonencaptured fluorescent probe was removed by gel filtration chromatography using Sephadex G-50 spin columns with an overall column yield of >85% (Pick, 1981). The resultant large unilamellar vesicles comprised of each phospholipid subclass were diluted with isoosmotic buffer (109 mM $(CH_3)_4NCl$, 4 mM MOPS, 2 mM Tris·Cl, 4 μM EDTA, 200 mM NaCl or KCl for Na^+ or Cl^- mobility measurements, respectively). The fluorescence emission from SBFI or PBFI probes was measured immediately upon the addition of

valinomycin utilizing a 470 nm cutoff filter with excitation wavelengths of 345 and 350 nm (8 nm slit width) and emission wavelengths of 515 and 508 nm (8 nm slit width) for SBFI and PBFI, respectively. The influx rate constants (κ) of valinomycin-mediated Na^+ transport or passive Cl^- movement were quantitated from alterations in the emission intensity (I) of fluorescent probes (SBFI or PBFI), where I depends hyperbolically on the concentration (C) of the cognate ion as

$$I = I_0 + \frac{\alpha P_T}{1 + K_{eq}/C}$$

where I_0 is the baseline intensity, α is a proportionality coefficient, P_T is the total probe concentration, and K_{eq} is the dissociation constant of the ion−probe complex (Jezek et al., 1990). Since the driving force for ion transport by valinomycin is the concentration gradient of each ion across the membrane, the expression for permeability is reduced to a simple first-order exponential relationship, as the captured probe is only sensitive to the specific ion, and, initially, that ion is only present outside the vesicle: $C = C_0(1-e^{-\kappa t})$ where C and C_0 are the concentrations inside and outside the vesicle, respectively, and κ is the diffusion rate constant related to the permeability (P) as $P = \kappa r/3$ (Ting et al., 1981; Mimms et al., 1981). The vesicle radii were 50 nm under the experimental conditions employed. The relationship between fluorescence intensity (I) and the diffusion rate constant (κ) can be summarized through the relationship

$$I = I_0 + \frac{1}{k_1 + \frac{1}{k_2 - k_3 e^{-\kappa t}}}$$

where k_1, k_2, and k_3 are proportionality coefficients. Temporal alterations in fluorescence intensity were analyzed by the above equation to derive both the diffusion rate constants and the corresponding permeability coefficients.

RESULTS AND DISCUSSION

Vesicles comprised of each of the three major choline glycerophospholipid subclasses (i.e., containing acyl, alkyl ether, or vinyl ether constituents at the *sn*-1 position, arachidonic acid esterified at the *sn*-2 position, and a phosphocholine polar head group at the *sn*-3 position) (Figure 1) were prepared and purified by gel filtration chromatography, and a K^+ gradient was generated across their membrane bilayers by dilution into isoosmotic buffer. As anticipated, addition of the potential-sensitive dye, 3,3′-dipropylthiadicarbocyanine iodide (diS-C_3-(5)), resulted in a time-dependent decrease in fluorescence intensity at 670 nm due to the progressive association of the dye with membrane until its new steady-state level was reached (Sims et al., 1974; Waggoner, 1976; Guillet & Kimmich, 1981). The subsequent addition of valinomycin resulted in the generation of an electrochemical gradient across the membrane bilayer and the rapid accumulation of dye within the membrane to its new potential-sensitive equilibrium concentration as demonstrated by a rapid increase in fluorescence quenching (Sims et al., 1974; Waggoner, 1976; Guillet & Kimmich, 1981; Cabrini & Verkman, 1986). Due to the ability of valinomycin to facilitate transmembrane K^+ flux, K^+ follows its concentration gradient after the addition of valinomycin and leaves the intravesicular space. Accordingly, the time-dependent dissipation of membrane potential can be quantified by measuring the resultant fluorescence dequenching as dye is released from the membrane and allowed to reach its new steady-state distribution at each transmembrane potential (Corda et al., 1982). Through comparisons of the rate of dye redistribution (i.e., fluorescence dequenching), alterations in valinomycin-facilitated K^+ flux can be quantified and the ability of each phospholipid subclass to facilitate valinomycin-mediated ion transport can be assessed. Valinomycin-mediated K^+ efflux was 2.7-fold larger in plasmenylcholine membranes in comparison to membranes comprised of either phosphatidylcholine or plasmanylcholine (Figure 2, Table 1). In this system, the rank order of valinomycin-mediated K^+ efflux in each choline glycerophospholipid subclass was plasmenylcholine > phosphatidylcholine ≈ plasmanylcholine. Furthermore, we demonstrated that the observed dissipation of the K^+ gradient cannot occur without the concomitant counterflow of Na^+ via the valinomycin carrier since, when lithium was utilized as the counterion in the extravesicular space, no dissipation of the membrane potential was present during the time course of the experiments (Figure 2). Thus, the

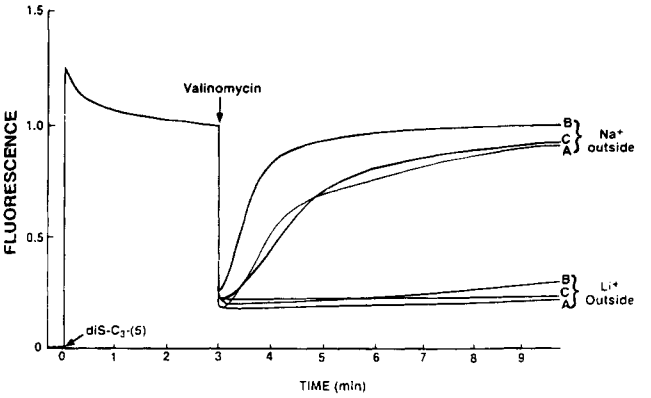

FIGURE 2: Subclass-mediated alterations in the kinetics of valinomycin-facilitated potential dissipation. Small unilamellar vesicles (d = 30 nm) comprised of 16:0−20:4 phosphatidylcholine (A), 16:0−20:4 plasmenylcholine (B), or 16:0−20:4 plasmanylcholine (C), prepared in K^+ medium (225 mM K_2SO_4, 50 mM KH_2PO_4−K_2HPO_4, pH 6.7 at 25 °C) as described in Materials and Methods were diluted with either Na^+-containing buffer (225 mM Na_2SO_4, 50 mM NaH_2PO_4−Na_2HPO_4, pH 6.7 at 25 °C) or isoosmotic Li^+-containing buffer (266 mM Li_2SO_4, 18 mM LiCl, pH 6.7 at 25 °C), resulting in the generation of an inward 100 mV potential after addition of valinomycin. To the liposomal suspension (50 μg lipid/mL) incubated at 25 °C, the potential-sensitive fluorescent dye, diS-C_3-(5) (dissolved in 7 μL of ethanol) was added prior to the addition of valinomycin (final concentration, 1.0×10^{-6} M). Fluorescence emission was monitored at 670 nm with excitation at 622 nm.

Table 1: Quantitation of the Rate Constants of Valinomycin-Mediated K^+/Na^+ Exchange in Each Phospholipid Subclass[a]

sample	$\kappa \times 10^2$ (1/s)
16:0−20:4 plasmenylcholine	6.1 ± 0.7
16:0−20:4 phosphatidylcholine	2.3 ± 0.5
16:0−20:4 plasmanylcholine	1.9 ± 0.2

[a] Rates of K^+/Na^+ exchange were calculated from the slope of initial potential dissipation in Figure 2 as stated in Materials and Methods. Values shown represent the mean ± SEM of at least four independent experiments.

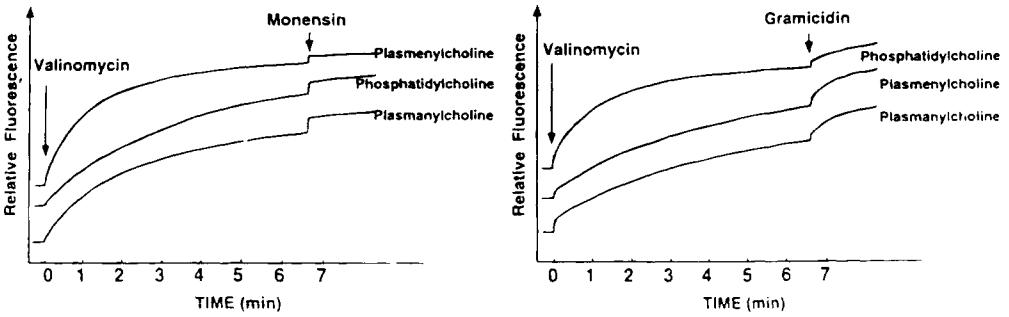

FIGURE 3: Phospholipid subclass-induced alterations in valinomycin-mediated ion influx. Large unilamellar vesicles (d = 100 nm) were prepared in buffer (300 mM $(CH_3)_4NCl$, 10 mM MOPS, 5 mM Tris·Cl, and 0.01 mM EDTA, pH 7.0 at 25 °C) containing either 300 μM SBFI (left panel) or PBFI (right panel) as previously described (Hope et al., 1985). Nonencaptured fluorescent probe was removed by gel filtration chromatography using Sephadex G-50 spin columns. Vesicles comprised of 16:0−20:4 phosphatidylcholine, 16:0−20:4 plasmenylcholine or 16:0−20:4 plasmanylcholine were diluted into isoosmotic buffer (109 mM $(CH_3)_4NCl$, 4 mM MOPS, 2 mM Tris·Cl, 4 μM EDTA) containing either 200 mM NaCl (left panel, for Na^+ mobility measurements) or 200 mM KCl (right panel, for Cl^- permeability measurements), and alterations in fluorescence intensity as a function of time after the addition of valinomycin were recorded. At the completion of the experiment, either 5 μM monensin or 1 μM gramicidin was added to the lipid suspension to facilitate complete distribution of residual Na^+ or K^+ gradients, respectively, for normalization. Fluorescence emission of SBFI or PBFI was measured through a 470 nm cutoff filter with excitation wavelengths of 345 and 350 nm and emission wavelengths of 515 and 508 nm, respectively. Left panel: Na^+ was present outside of vesicles (2250 μg lipid/mL), and valinomycin (1.9×10^{-5} M) was added where indicated. Right panel: K^+ was present outside of vesicles, suspensions contained 900 μg lipid/mL, and valinomycin (3.8×10^{-7} M) was added where indicated.

observed potential dissipation reflects valinomycin-mediated K^+/Na^+ exchange and the calculated rate constants reflect valinomycin-mediated K^+/Na^+ exchange in each phospholipid subclass. Furthermore, since valinomycin-mediated ion transport is selective for K^+ ion in comparison to Na^+ ion, the measured rate of ion transport is limited by the rate of Na^+ transport across the membrane bilayer.

To directly examine the effects of each phospholipid subclass on valinomycin-mediated Na^+ transport, we utilized the sodium ion-selective probe, SBFI. Vesicles comprised of each of the three choline glycerophospholipid subclasses (i.e., containing arachidonic acid at the *sn*-2 position and a choline polar head group at the *sn*-3 position) were prepared in the presence of SBFI, and the nonencapsulated probe was subsequently removed by gel filtration chromatography. The ability of valinomycin to function as a Na^+ carrier was assessed by quantification of alterations in the fluorescence intensity of the SBFI probe as a function of time after the addition of an appropriate amount of valinomycin (1.9×10^{-5} M) for which membrane Cl^- permeability was not rate-limiting for Na^+ transport. Vesicles comprised of plasmenylcholine facilitated valinomycin-mediated Na^+ transport to a greater extent than did vesicles comprised of either phosphatidylcholine or plasmanylcholine (Figure 3, Table 2).

To further elucidate the functional sequelae underlying the enrichment of plasmalogens in electrically-active membranes, we examined the passive membrane properties of vesicles comprised of each subclass by quantifying the rate of Cl^- influx into the vesicle interior. The potassium ion-selective probe, PBFI, was utilized to measure Cl^- influx by quantitation of the temporal dependence of alterations in its fluorescence intensity in vesicles comprised of each phospholipid subclass. Since the ratio of the membrane permeability of K^+ to Cl^- is greatly increased when valinomycin is introduced as a substitutional impurity into the membrane bilayer (Hoffman & Laris, 1974), the initial rapid influx of potassium ion into the vesicle (leaving the relatively impermeable chloride ion outside the vesicles) results in the generation of charge separation which attenuates the additional entrance of K^+ into the vesicle interior. At time points >2 s, the K^+ subsequently follows the movement of Cl^- to the inside of vesicles as demonstrated by the time-dependent increase in fluorescence intensity. Thus, the observed K^+ influx during the second stage is a measure of the passive Cl^- mobility across the membrane bilayer. Passive Cl^- permeability in vesicles comprised of phosphatidylcholine was over 4-fold greater than that manifest by vesicles comprised of plasmenylcholine. The rank order of Cl^- permeability for each phospholipid subclass was phosphatidylcholine > plasmenylcholine ≈ plasmanylcholine (Figure 3, Table 2).

Collectively, these results demonstrate substantial differences in both the ionophore-mediated and passive ion transport properties of vesicles comprised of each phospholipid subclass. To elucidate the molecular mechanisms underlying these effects, it is first important to consider the rate-determining components of each transport process. Valinomycin-mediated ion transport is a multistep process comprised of at least four discrete steps including (1) ion association with valinomycin at the membrane−solution interface, (2) translocation of the ion−valinomycin complex across the lipid bilayer to the opposite interface, (3) dissociation of the valinomycin−ion complex and release of the ion into solution, and (4) back transport of free valinomycin carrier to the initial state (Stark et al., 1971; Läuger, 1972). It has been previously shown that both association and dissociation of ion with valinomycin are rapid processes and that the rate-determining step for valinomycin-mediated ion transport is the translocation of the ion−valinomycin complex across the membrane bilayer (Benz et al., 1973; Block et al., 1974; Läuger et al., 1981). This valinomycin-mediated translocation process across the membrane involves at least three distinct components including (1) the departure of the valinomycin−ion complex from the membrane interface, (2) the translocation of the complex across the hydrophobic membrane, and (3) the association of the ion complex at the opposite interface preceding release of ion. The departure of the valinomycin−ion complex from the membrane interface and its transport to the membrane interior is initiated through the ablation of stabilizing interactions between the valinomycin-bound K^+ (or Na^+) and the

Table 2: Rate Constants and Permeability Coefficients of Na^+ or Cl^- Flux in Each Phospholipid Subclass[a]

	Na^+		Cl^-	
sample	$\kappa \times 10^4$ (1/s)	$P \times 10^{10}$ (cm/s)	$\kappa \times 10^4$ (1/s)	$P \times 10^{10}$ (cm/s)
16:0−20:4 plasmenylcholine	2.5 ± 0.1	4.2 ± 0.2	0.6 ± 0.2	1.0 ± 0.3
16:0−20:4 phosphatidylcholine	1.3 ± 0.3	2.2 ± 0.5	2.6 ± 0.4	4.3 ± 0.7
16:0−20:4 plasmanylcholine	1.3 ± 0.1	2.2 ± 0.2	0.8 ± 0.1	1.3 ± 0.2

[a] The influx rate constants of Na^+ via valinomycin carriers or passive Cl^- movement were quantitated utilizing changes in the intensity of the fluorescent probes SBFI or PBFI, respectively. Time courses of alterations in fluorescence intensity in Figure 3 were fitted according to the algorithm in Materials and Methods to derive diffusion rate constants (κ) and the corresponding permeability coefficients (P). Values shown represent the mean ± SEM of at least three independent experiments.

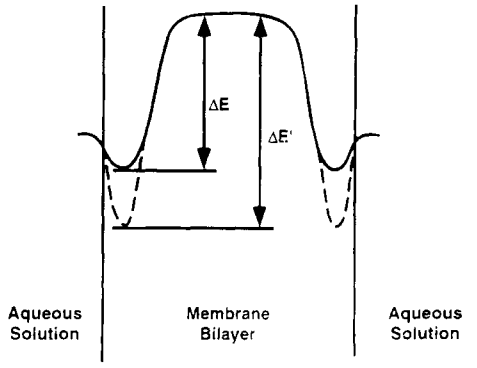

FIGURE 4: Schematic representation of the free energy profile of valinomycin-mediated ion transport across a lipid bilayer. ΔE indicates the energy barrier for carrier-mediated transport in plasmenylcholine membranes while $\Delta E'$ indicates the energy barrier for transport of the ion−carrier complex in either phosphatidylcholine or plasmanylcholine membranes where substantial interfacial stabilization of the valinomycin−ion complex (mediated by the ester or alkyl ether linkages present in the *sn*-1 position) can occur. We point out that other factors including alterations in interfacial dipole potential, conformation of the carbonyls in each phospholipid subclass, and alterations in membrane physical properties may also contribute to subclass-specific alterations in energy profiles as described in the text.

heteroatoms at the membrane interface. The electron-donating propensities of both ester and alkyl ether linkages in bilayers substantially exceed that of the vinyl ether linkage due to the reasonance effect of the nonbonding electron pair of O with the π-orbital in the olefinic linkage (Ingold & Ingold, 1926). Accordingly, the proximal portion of the *sn*-1 aliphatic chain in both phosphatidylcholine and plasmanylcholine can stabilize the valinomycin−ion complex, while such stabilization is anticipated to be minimal or absent in interactions with the vinyl ether constituent. Thus, the net energy barrier (ΔE in Figure 4) for the process of transbilayer movement would be substantially smaller in plasmenylcholine-containing membranes since less stabilization of the interfacial valinomycin−K^+ (or Na^+) is present at the membrane interface and the energy of the transition state in the hydrophobic membrane interior is similar for each choline glycerophospholipid subclass since they are comprised of identical aliphatic constituents. We point out that other factors including, but not limited to, alterations in membrane dipole potential, conformational alterations of the hetero-atoms during cation chelation, and subclass specific changes in the physical properties of the membrane could also contribute to the observed alterations in valinomycin-mediated ion flux. The sum total effect resulting from each of these factors is to decrease the residence time of the valinomycin−K^+ (or Na^+) complex at the interface of plasmenylcholine membranes and thereby increase the rate of ionophore-mediated ion transport.

In regard to passive ion transport, we point out that the surface dipole moment of phosphatidylcholine is substantially larger than that of plasmenylcholine membranes (Shah & Schulman, 1965; Smaby et al., 1983). This has been attributed to the presence of the vertically oriented double bond vicinal to the ether oxygen in plasmalogens and to the large contribution that the carbonyls make to the net dipole moment (Shah & Schulman, 1965; Paltauf et al., 1971). The relatively larger interfacial dipole potential in phosphatidylcholine membranes can increase the partition coefficient of Cl^- into the membrane bilayer (Andersen et al., 1976; Honig et al., 1986; Flewelling et al., 1986; Franklin et al., 1993) resulting in a substantial acceleration of passive Cl^- transport. Furthermore, the molecular conformation and dynamics of plasmalogen and diacyl phospholipids are substantially different (Malthaner et al., 1987; Pak et al., 1987; Han & Gross, 1990; Chen et al., 1993). Specifically, plasmenylcholine membrane bilayers are much more densely packed than diacyl phospholipids (Smaby et al., 1983) since they do not contain a kink in the proximal portion of the *sn*-2 aliphatic chain (Han & Gross, 1990). Thus, the increase of the Cl^- partition coefficient into the diacylphosphatidylcholine in conjunction with the reduction of Cl^- mobility in plasmalogen membranes account for a 4-fold increase in Cl^- permeability in phosphatidylcholine membranes in comparison to plasmenylcholine membranes. The present data quantifying passive Cl^- transport does not agree with published data by Hermetter & Paltauf (1981) which ranks the choline subclasses: alkyl acyl > alkenyl acyl > diacyl. The differences between that study and the present investigation may be due to the use of heterogeneous mixtures of lipid constituents as well as the presence of a different fatty acid (oleic acid) incorporated at the *sn*-2 position in the prior study. We point out that the rank order of Cl^- transport reported by Hermetter & Paltauf (1981) does not agree with the prediction by Andersen et al. (1976) that increased surface dipole potential can increase the partition coefficient of anions into membranes and hence increase passive anion transport. In contrast, the results of the present study demonstrating increased passive Cl^- permeability in membranes comprised of phosphatidylcholine in comparison to membranes comprised of plasmenylcholine are consistent with the prediction by Anderson et al. (1976).

Thus, the function of plasmalogens in electrically-active membranes is likely 3-fold. First, the diminished electron-donating properties manifest by the proximal portion of aliphatic chains in plasmenylcholine membranes accelerate the rate of carrier-mediated cation transport. Second, the differential interfacial dipole potential in membranes comprised of plasmenylcholine compared to phosphatidylcholine can provide the increased capacitance (decreased passive membrane permeability) necessary for the optimization of electrical conduction. Third, the altered molecular geometry, membrane dynamics, and increased packing efficiency in membranes comprised of plasmalogen molecular species

establish an enhanced permeability barrier to attenuate the rate of passive ion flux. Thus, through the interplay of subclass-specific stereoelectronic characteristics, membrane physical properties, membrane molecular dynamics, and the unique conformational motifs inherent in the covalent structure of plasmalogen molecular species, the delicate integration of lipid structure and function in electrically-active membrane bilayers is achieved.

REFERENCES

Andersen, O. S., Finkelstein, A., Katz, I., & Cass, A. (1976) *J. Gen. Physiol. 67*, 749−771.

Bayon, Y., Croset, M., Chirouze, V., Tayot, J. L., & Lagarde, M. (1993) *Lipids 28*, 631−636.

Benz, R., Stark, G., Janko, K., & Läuger, P. (1973) *J. Membr. Biol. 14*, 339−364.

Block, M. C., DeGier, J., & Van Deenen, L. L. M. (1974) *Biochim. Biophys. Acta 367*, 210−224.

Cabrini, G., & Verkman, A. S. (1986) *J. Membr. Biol. 90*, 163−175.

Chen, X., Han, X. & Gross, R. W. (1993) *Biochim. Biophys. Acta 1149*, 241−248.

Corda, D., Pasternak, C., & Shinitzky, M. (1982) *J. Membr. Biol. 65*, 235−242.

Creer, M. H., & Gross, R. W. (1985) *J. Chromatogr. 338*, 61−69.

Flewelling, R. F., & Hubbell, W. L. (1986) *Biophys. J. 49*, 531−540.

Franklin, J. C., Cafiso, D. S., Flewelling, R. F., & Hubbell, W. L. (1993) *Biophys. J. 64*, 642−653.

Gross, R. W. (1984) *Biochemistry 23*, 158−165.

Gross, R. W. (1985) *Biochemistry 24*, 1662−1668.

Gross, R. W. (1992) *Trends Cardiovasc. Med. 2*, 115−121.

Guillet, E. G., & Kimmich, G. A. (1981) *J. Membr. Biol. 59*, 1−11.

Han, X., & Gross, R. W. (1990) *Biochemistry 29*, 4992−4996.

Han, X., Zupan, L. A., Hazen, S. L., & Gross, R. W. (1992) *Anal. Biochem. 200*, 119−124.

Hermetter, A., & Paltauf, F. (1981) *Chem. Phys. Lipids 29*, 225−233.

Hoffman, J. F., & Laris, P. C. (1974) *J. Physiol. 239*, 519−552.

Honig, B. H., Hubbell, W. L., & Flewelling, R. F. (1986) *Annu. Rev. Biophys. Biophys. Chem. 15*, 163−193.

Hope, M. J., Bally, M. B., Webb, G., & Cullis, P. R. (1985) *Biochim. Biophys. Acta 812*, 55−65.

Ingold, C. K., & Ingold, E. H. (1926) *J. Chem. Soc.* 1310−1328.

Jezek, P., Mahdi, F., & Garlid, K. D. (1990) *J. Biol. Chem. 265*, 10522−10526.

Johnston, N. C., & Goldfine, H. (1992) *J. Bacteriol. 174*, 1848−1853.

Karnovsky, M. J., Kleinfeld, A. M., Hoover, R. L., & Klausner, R. D. (1982) *J. Cell Biol. 94*, 1−6.

Läuger, P. (1972) *Science 178*, 24−30.

Läuger, P., Benz, R., Stark, G., Bamberg, E., Jordan, P. C., Fahr, A., & Brock, W. (1981) *Q. Rev. Biophys. 14*, 513−598.

MacDonald, J. I., & Sprecher, H. (1989) *J. Biol. Chem. 264*, 17718−17726.

Malthaner, M., Hermetter, A., Paltauf, F., & Seelig, J. (1987) *Biochim. Biophys. Acta 900*, 191−197.

Masuda, M., Kudo, I., Naito, M., Mizushima, H., & Inoue, K. (1991) *Biochim. Biophys. Acta 1083*, 235−242.

Mimms, L. T., Zampighi, G., Nozaki, Y., Tanford, C., & Reynolds, J. A. (1981) *Biochemistry 20*, 833−840.

Pak, J. H., Bork, V. P., Norberg, R. E., Creer, M. H., Wolf, R. A., & Gross, R. W. (1987) *Biochemistry 26*, 4824−4830.

Paltauf, F., Hauser, H., & Phillips, M. C. (1971) *Biochim. Biophys. Acta 249*, 539−547.

Pick, U. (1981) *Arch. Biochem. Biophys. 212*, 186−194.

Ramesha, C. S., & Pickett, W. C. (1987) *J. Lipid Res. 28*, 326−331.

Shah, D. O., & Schulman, J. H. (1965) *J. Lipid Res. 6*, 341−349.

Shaikh, N. A. (1990) *Mol. Cell Biochem. 96*, 43−55.

Sims, P. J., Waggoner, A. S., Wang, C., & Hoffman, J. F. (1974) *Biochemistry 13*, 3315−3330.

Smaby, J. M., Hermetter, A., Schmid, P. C., Paltauf, F., & Brockman, H. L. (1983) *Biochemistry 22*, 5808−5813.

Stark, G., Ketterer, B., Benz, R., & Läuger, P. (1971) *Biophys. J. 11*, 981−994.

Takamura, H., Kasai, H., Arita, H., & Kito, M. (1990) *J. Lipid Res. 31*, 709−717.

Ting, D. Z., Hagan, P. S., Chan, S. I., Doll, J. D., & Springer, C. S. (1981) *Biophys. J. 34*, 189−215.

Tshinaga, M., Tanimoto, M., Sugiyama, S., Kumamoto, R., & Yokoro, K. (1991) *Biochem. Cell Biol. 69*, 655−660.

Waggoner, A. (1976) *J. Membr. Biol. 27*, 317−334.